



Published in final edited form as:

Mol Imaging Biol. 2023 February ; 25(1): 156–167. doi:10.1007/s11307-021-01699-6.

Effects of Light Absorbing Carbons in Intra-Operative Molecular Imaging Guided Lung Cancer Resections

Feredun Azari, MD¹, Gregory Kennedy, MD¹, Kevin Zhang, BA¹, Elizabeth Bernstein, BA¹, Ashley Chang, BS¹, Bilal Nadeem, BA¹, Alix Segil, BA¹, Charuhas Desphande, MD³, James Delikatny, PhD², John Kucharczuk, MD¹, Sunil Singhal, MD¹

¹Department of Thoracic Surgery, University of Pennsylvania Perelman School of Medicine, Philadelphia, PA

²Department of Radiology, University of Pennsylvania Perelman School of Medicine, Philadelphia, PA

³Department of Pathology, University of Pennsylvania Perelman School of Medicine, Philadelphia, PA

Abstract

Background: One of the novel advancements to enhance the visual aspects of lung cancer identification is Intraoperative Molecular Imaging (IMI), which can reliably detect tumors that would otherwise be missed by standard techniques such as tactile and visual feedback, particularly for sub centimeter or ground-glass nodules. However, there remains a subset of patients who do not benefit from IMI due to excessive background fluorescence secondary to parenchymal light-absorbing carbon deposition. Our goal was to identify the effects of these carbonaceous materials on the quality of IMI guided lung cancer resections.

Study Design and Methods: Between July 2014 and May 2021, a total of 311 patients were included in the study. Patients underwent infusion of the study drug OTL38 or ICG up to 24 hours prior to VATS for lung cancer. Several factors such as age, tumor subtype, PET SUV, smoking, demographics, chronic lung conditions, patient domicile, and anthracosis were analyzed with respect to lung fluorescence during IMI. P values <0.05 were considered statistically significant.

Results: Variables such as age, sex, and race had no statistical correlation to IMI success. However, smoking status and pack year had statistically significant correlation with background parenchymal fluorescence and lung inflammation ($p < 0.05$). MFI of background (lung parenchyma) correlated with smoking history ($p < 0.05$) which led to decreased tumor-to-background ratio (TBR) measurements for all patients with proven malignancy ($p < 0.05$). Patients with chronic lung disease appear to have increased background parenchymal fluorescence regardless of smoking history (287 vs 154, $p < 0.01$). City dwellers compared to other groups appear to be exposed to higher pollutant load and have higher rates of anthracosis but living location's impact on fluorescence quantification appears to be not statistically significant.

Corresponding Author: Sunil Singhal, M.D, Department of Thoracic Surgery, Hospital of the University of Pennsylvania, 3400 Spruce Street, 6 White Building, Philadelphia, PA, 19104, sunil.singhal@pennmedicine.upenn.edu.

Conflict of Interest: Authors report no conflict of interest.

Conclusion: Smokers with greater than 10 PPY and those with chronic lung disease appear to have decreased lesion to background discrimination, significant anthracosis, and reduced IMI efficacy secondary to light-absorbing carbon deposition.

Introduction:

Complete oncologic pulmonary resection is paramount for successful outcomes early-stage non-small cell lung cancer¹. During resection, thoracic surgeons rely on visual and tactile feedback to ensure that the lung and thoracic cavity are appropriately evaluated. However, as the field of thoracic surgery undergoes a renaissance with minimally invasive options, the surgeon's ability to use tactile clues has diminished causing intraoperative decision making to be heavily dependent on visual appearances².

One of the novel advancements to enhance the visual aspects of lesion identification is intraoperative molecular imaging (IMI)³. This technology utilizes specialized near-infrared (NIR) contrast agents injected intravenously into patients prior to surgery and target receptors on tumors and highlight cancer cells real time. Previous research has found that IMI can reliably identify primary and occult tumors better than current standard techniques⁴⁻⁶. Several tracers such as OTL38 (folate receptor targeted), indocyanine green (ICG), SGM-101 (CEA targeted), EC-17 (Folate) along with others have been shown to be effective⁶⁻⁸. However, there remains a subset of patients who do not benefit from IMI despite confirmation of the targeted receptor expression.

We hypothesized one of the explanations for significant visual noise during IMI is lung anthracosis. In patients with significant tobacco and environmental exposures, the lungs develop anthracosis (ie. darkened, black lungs), thus, visual assessment of the lung can be challenging⁹⁻¹¹. We predicted anthracotic lungs are difficult to visually assess using visual cues by white light and fluorescence guided surgery. These excitation wavelengths (white light 400-700 nm; NIR light 700-900 nm) cannot penetrate deep to anthracotic pigmentation¹². The highly pigmented anthracotic nodules tend to absorb all white light which reduces parenchymal visibility. Even when IMI fluorescence is utilized, the dark pigment generated from years of soot and particulate deposition produces a parenchymal inflammation that makes it challenging to differentiate inflamed lung from a cancerous lesion.

Currently, there are limited reliable objective means of assessing the degree of anthracosis a patient may have. Cross sectional imaging, serum markers, and respiratory function do not necessarily assess the soot deposition into the parenchyma. Since anthracosis is intimately related to long duration of environmental exposures⁹, our goal in this study was to assess if social determinants of health such as smoking history, domicile (urban vs suburban vs rural dwelling), chronic lung disease, and demographics can predict anthracosis and failure of IMI. We hypothesize that those with significant smoking history, lung damage from chronic respiratory diseases, and patient living location can predict lung anthracosis and may decrease the utility of IMI.

Methods:

Data Collection:

Appropriate authorization was obtained from the University of Pennsylvania Institutional Review Board. Data was retrospectively analyzed from a prospectively collected database. Between July 2014 and May 2021, a total of 311 patients were included in the study of whom 279 had complete clinical data for data analysis. Based on institutional practice patterns, pre-operative tissue sampling and diagnosis was not mandatory. Selected patients underwent appropriate pre-operative clearance prior to operative scheduling with video-assisted thoracoscopic surgical (VATS) lobectomy being the procedure of choice.

Inclusion Criteria: Patients underwent a thorough pre-operative evaluation and risk stratification with fine cut CT scanning and PET/CT for additional synchronous lesions and extra-pulmonary disease sites. Patients with no additional lesions (both intra and extra-pulmonary) and deemed appropriate for curative resection were then consented for IMI-guided surgery which included anatomic oncologic resection for primary lung malignancy. Inclusion criteria included male and female patients 18 years of age and older with confirmed diagnosis of adenocarcinoma lung cancer for OTL38 studies or have a primary diagnosis, or at high clinical suspicion, of lung nodule(s) warranting surgery based on CT and/or PET imaging for ICG guided IMI. Additionally, a negative serum pregnancy test at screening followed by a negative urine pregnancy test on the day of surgery or day of admission for female patients of childbearing potential, female patients of childbearing potential or less than 2 years postmenopausal agree to use an acceptable form of contraception from the time of signing informed consent until 30 days after study completion, ability to understand the requirements of the study, provide written informed consent and authorization of use and disclosure of protected health information, and agree to abide by the study restrictions and to return for the required assessments.

Exclusion Criteria: Exclusion criteria for enrollment in the studies included: previous exposure to fluorescent tracers, any medical condition that in the opinion of the investigators could potentially jeopardize the safety of the patient, history of anaphylactic reactions or severe allergies, history of allergy to any of the components of OTL38 or ICG, including folic acid, pregnancy, or positive pregnancy test, clinically significant abnormalities on electrocardiogram (ECG) at screening, presence of any psychological, familial, sociological or geographical condition potentially hampering compliance with the study protocol and follow-up schedule, impaired renal function defined as estimated glomerular filtration rate (eGFR) < 50 mL/min/1.73m², Impaired liver function defined as values > 3x the upper limit of normal for alanine aminotransferase (ALT) or aspartate aminotransferase (AST), alkaline phosphatase (ALP), or total bilirubin, received an investigational agent in another investigational drug or vaccine trial within 30 days prior to surgery, known sensitivity to fluorescent light.

Surgical Procedure and NIR Tracer: Analyzed patients underwent infusion of the study drug OTL38 (On Target Laboratories, West Lafayette, Indiana) or ICG (Akorn Pharmaceuticals, Decatur, Illinois), up to 24 hours prior to surgery. OTL38 is a folate

analog conjugated to the NIR dye, S0456 which excites at 774–776nm and emits at 794–796nm. OTL38 targets folate receptor alpha, which is expressed in more than 90% of adenocarcinomas of the lung¹³. ICG is an FDA approved NIR tracer with similar emission and excitation to that of S0456 but utilizes leaky capillaries of the tumor microenvironment via enhanced permeability and retention effect.

During pulmonary resection, surgeons utilized bright field imaging and finger palpation through port site incisions to confirm the lesions in the anatomical location of interest.

Camera Systems

In situ, fluorescent imaging was performed using VisionSense Iridium (Medtronic, Minneapolis, MN) imaging system. VisionSense Iridium IMI based optical devices are high definition, dual band (white light and NIR) camera systems capable of concurrent NIR emission and detection. The tracer specific Iridium system utilizes an excitation laser with a wavelength of 780-805nm, with fluorescence detection based on a bandpass filter selective to light ranging from 790- 850 nm. VisionSense Iridium uses two charge-coupled device sensors to produce simultaneous white-light RGB and NIR fluorescence images from the emission channel and merges the two in real time¹⁴. It is coupled to a dedicated 4-mm outer diameter endoscope and exoscope attachment that allowed for wider visualization area. Both endoscope and exoscope attachments have a dual optical path design that enables the separate use of white light (visible light) and NIR light¹⁵. Complete details of the VisionSense system are shown in Supplementary Table 1.

Patients who underwent OTL38 guided lung cancer resections were imaged by an OTL38 calibrated imaging device whereas the ICG group were imaged by ICG calibrated imaging systems.

The lungs and the tumor were imaged prior to resection without any surgical manipulation. Fluorescence parameters were measured for unresected tumors and lung parenchyma in order to minimize artificial darkening of the lung parenchyma secondary to venous congestion.

IMI based optical devices are high definition, dual band (white light and NIR) camera systems capable of concurrent NIR emission and detection. The tracer specific Iridium system utilizes an excitation laser with a wavelength of 780-805nm, with fluorescence detection based on a bandpass filter selective to light ranging from 790- 850 nm. Patients who underwent OTL38 guided lung cancer resections were imaged by OTL38 calibrated imaging device whereas the ICG group were imaged by ICG calibrated imaging systems

Location and Air Quality Index:

Demographic distribution of patient population treated at UPHS facilities were mapped using the publicly available mapping tool from randymajors.org. Air Quality Index (AQI) for various locations of interest were obtained from the publicly available database from the Environmental Protection Agency (EPA). According to the agency: The AQI is a nationally uniform color-coded index developed by EPA for reporting and forecasting daily air quality. The AQI reports the most common ambient air pollutants that are regulated under the Clean

Air Act, including ozone and particle pollution (PM₁₀ and PM_{2.5}). AQI index ranges from 0 to 500. Values 50 or below represents good air quality whereas values greater than 300 are considered hazardous. PM(2.5) levels obtained from the EPA database were used as the degree of pollutant exposure as these substances given their small size are able to enter the respiratory system.

Specimen Analysis, TBR Calculation, Definitions:

Mean Fluorescence Intensity (MFI) of the tumors and normal lung parenchyma were calculated using ImageJ (National Institutes of Health) and MATLAB (Mathworks, Natick, MA) softwares with minimum 1000 pixels being included. Tumor-to-background ratios (TBR) were calculated for the specimens. Both parametric and non-parametric statistical analyses were performed using SPSS version 27 (IBM Technologies). p values <0.05 were considered statistically significant.

Definitions: Fluorescence (Fluorescence Intensity): Refers to quantification of fluorescence detected by the NIR camera and measured by image analysis software mentioned above. Parameters used for quantification include Tumor to Background Ratio (TBR), Mean Fluorescence Intensity. Unless mentioned specifically mentioned, MFI values are used for comparison of fluorescence intensity between two samples

Degree of Background Inflammation: refers to non-specific fluorescence detected from the uninvolved (by pathology) of the lung and are measured as MFI values calculated using image analysis software mentioned above.

Background Fluorescence: refers to non-specific fluorescence of the lung detected in patients who did not receive NIR imaging agent (ICG or OTL38) and are measured as MFI values calculated using image analysis software mentioned above. No TBR measurements performed in this cohort as these patients did not receive targeted agents (i.e tumor not expected to fluoresce).

Anthracosis: degree of anthracosis refers to “darkness” of lungs as perceived by the observers. In order to standardize degree of lung anthracosis, 100 in-situ images were shown to 5 independent observers who were asked to characterize lungs. Based on the survey: 0 was no to minimal anthracosis (pink parenchyma throughout, example Figure 2-A Right Column), 1+ anthracosis: mild soot deposition seen throughout the lung with pink parenchyma noted in-between soot laden lung parenchyma (Example Figure 2-A middle column) , 2+: significant anthracosis: soot laden lung parenchyma with no to minimal normal parenchyma intertwined between the soot depositions (Example Figure 2-A left column)

Results:

Demographics:

Of the 279 patients analyzed In the cohort, >60% of the patients were female. Mean age of the cohort was 64.1 years. Approximately 30% of patients were from the city of Philadelphia, 34% were from surrounding suburbs within the state of Pennsylvania, 18.7%

were from rural areas of Pennsylvania, 16.1 % were from adjacent counties in the states of New Jersey and Delaware, and 1.2% were from elsewhere not in the tri-state area. Geographical distribution is depicted in Figure 1. Table 1 shows demographic distribution of the cohort. Forty-seven percent of patients identified as white, 21% were black, 10% were Hispanic, 2.6 % as Asian, and 20% were unknown.

All patients during this time frame underwent successful infusion of NIR tracers within 24 hours with mean time to surgery from infusion of 17.23 hours (SD 5.3). 74 patients in the analysis underwent ICG infusion (~26%) and 251 (~74%) underwent OTL38 infusion. There were 17 adverse events related to tracer infusion none of which were severe and did not preclude subsequent scheduled surgical intervention. Summary of demographic and histopathologic patterns are presented in Table 1 and Supplementary Table 2, respectively

Anthracosis Related to Smoking History:

Analysis of demographics demonstrated that 39 patients were current smokers, 147 were past smokers, and 111 never smoked. Current smokers were more likely to be male ($p<0.05$) and have greater than 31.7 pack year (PPY) smoking history ($p<0.05$). As demonstrated in Figure 2-A and B, smoking status and pack year had statistically significant correlation with degree of background inflammation and parenchymal fluorescence with median smoker background MFI of 157 vs 21 in non-smokers ($p<0.05$). MFI of background (lung parenchyma) correlated with smoking history (Figure 2-B, $p<0.05$) for both the NIR tracers which led to decreased tumor-to-background ratio (TBR) measurements for all patients with histopathologically proven malignancy (Figure 2-B, (TBR 3.61 non-smokers vs 2.41 (median) smokers) OTL38, $p<0.05$)(2.89 vs 1.96 ($p<0.05$)ICG). Current smokers had the darkest lungs (2+ and 3+ anthracosis) with highest MFI compared to past smokers (267 vs 206)($p<0.05$). Subset analysis for both the tracers were done for adenocarcinoma spectrum lesions showing similar trends associated with increasing PPY.

Interestingly, past smokers who quit more than 10 years ago had no difference in parenchymal MFI and degree of background inflammation compared to never smokers (71 vs 21, $p=0.51$). 3-D analysis (Figure 2-C) showed that current smokers and those with past smoking history who quit less than 10 years ago with greater than 10 cumulative PPY had increased background signal intensity (i.e degree of background inflammation) (green and blue on RGB 3D scale) than those who never smoked ($p<0.05$). Topographic heat mapping of the tumor to background showed increased signal intensity in non-smokers compared to past smokers and current smokers ($p<0.05$). TBR analysis for lung adenocarcinoma patients who underwent OTL38 guided resections, showed non-anthroctic lungs in that cohort had higher TBR and lower background MFI compared to patients with anthracosis with background fluorescence signal intensity difference being statistically significant (102 vs 227 ($p<0.05$)). Table 3. Results from our analysis indicates that knowledge of smoking habits can inform the surgeon about appropriate counselling for IMI guided pulmonary tumor resection.

Background Lung Fluorescence in Non-Smokers

Chronic Lung Disease: 46 patients in the cohort had a diagnosis of chronic lung disease (both obstructive and restrictive) who did not have smoking history. While these patients had visibly non-anthracotic lung appearance (>95%, 44/46 had 1+ anthracosis), there was significant background parenchymal fluorescence and inflammation. Compared to patients without significant chronic lung disease, background MFI (degree of background inflammation) in these patients was statistically higher (287 vs 154, $p<0.01$). Tumor MFI difference was not statistically significant between the groups (613 vs 634, $p=0.17$). Increased degree of background inflammation did reduce the TBR measurements in the chronic lung disease group (2.11 vs 4.32, $p<0.05$). Increased background fluorescence intensity was noticed using the RGB 3D analysis and topographical 3D heat map (Figure 3). In summary, patients with chronic lung disease appear to have increased background parenchymal fluorescence regardless of smoking history.

Environmental Factors:

Given the diverse geographical background of the cohort, we analyzed the association of patient domicile with anthracosis, degree of background inflammation, and IMI fluorescence quantification. Air Quality Index (AQI) based on particulate matter with less than 2.5 micrometer diameter (PM_{2.5}) were obtained from the Environmental Protection Agency (EPA)¹⁶ (Supplemental Figure 1). City of Philadelphia and the immediate surrounding areas had the highest PM_{2.5} AQI in year 2020, highest average PM_{2.5} AQI over the last 5 years, and greatest maximal AQI over the last 20 years compared to rural areas, Philadelphia suburbs, and coastal areas. Patients from Atlantic city and surrounding areas had the lowest exposure to pollutants, had the lowest AQI>100 days, and lowest maximal PM_{2.5} AQIs. Patients from rural areas had higher exposure to pollutant particulate matter compared to those living in suburban areas. Spatial distribution of this patient population is demonstrated in Figure 1.

When accounting for confounders from smoking and chronic lung disease, patients living in a large metropolitan area tend to have greater anthracosis compared to those who live in coastal areas. There was no statistical difference between city dwellers and those who live in the suburban areas with respect to anthracosis, background MFI, and TBR calculations ($p=0.21$). However, patients from rural areas tended to have higher anthracosis compared to suburban regions. Rural areas had a statistically higher rate of smoking compared to suburban areas ($p<0.05$). In summary, city dwellers compared to other groups appear to be exposed to higher pollutant load and have higher rate of anthracosis but living location's impact fluorescence quantification appears to be not statistically significant (Figure 4).

Light Absorbing Carbon Fluorescence Without NIR Tracer Infusion—In order to understand the effects of LACs on background lung parenchymal fluorescence in anthracotic lungs without NIR tracer confounding, we explored MFI of lung parenchyma in patients who underwent standard of care surgery without IMI guidance (No NIR tracer infusion). In patients with 1+ and 2+ anthracosis, NIR bandpass filtered camera devices detected fluorescence in lung parenchyma (MFI 144 (27)) Figure 5. Interestingly, the areas without anthracosis did not have significant fluorescence detected Supplementary Video 1. Since the

observation that dark parenchyma with soot absorbs and emits NIR light, we explored if areas thermally coagulated during surgery for hemostasis subsequently fluoresced in patients who did not receive NIR infusion. The areas that were coagulated and produced charred tissue did fluoresce, particularly adipose and muscle tissue which do not fluoresce under normal situations regardless of NIR tracer (Figure 5)(Supplementary Video 2). In Summary, light absorbing carbons produce fluorescence in NIR IMI Guided lung cancer resections regardless of systemic NIR infusion.

Discussion:

Intraoperative molecular imaging (IMI) has the potential to transform the field of thoracic oncology over the coming years as more targeted tracers progress through the clinical trials^{5,17,18}. Utilization of various targeted NIR tracers can allow the physician to target sub-centimeter lesions, occult nodules, and assess the efficacy of the oncologic resection^{3,6}. However, as with all technologies, not every patient stands to benefit from IMI. We observed that those with particularly severe anthracosis, where it is difficult to discern the tumor visually, NIR detection of fluorescence can be particularly challenging. In this study we explored how social determinants of health can help the surgeon predict success of IMI guided lung cancer localization, degree of anthracosis, and background normal parenchymal fluorescence intensity limiting lesion differentiation.

Smoking has long been recognized as a carcinogen and one of the leading causes of lung cancer worldwide¹⁹. This patient population are an integral part every thoracic surgeon's practice and 186/279 (~66%) in this cohort had smoking history. The degree of smoking in our analysis has been shown to be correlated with increased anthracosis, increased background inflammation leading to decreased TBRs (Figure 2). All these findings in unison makes It harder for the surgeon to visualize tumor from normal parenchyma and renders IMI less effective.

Anthracosis generates a black pigment through deposition of carbonaceous particles such as soot^{9,20-22}. The term "soot" (also known as black carbon (BC) which refers to light-absorbing carbons) is used by the Intergovernmental Panel on Climate Change (IPCC) to denote light-absorbing combustion generated aerosols²³. In-depth analysis by Chakrabarty et al and Bond et al, have shown significant increased absorption of light and energy by exploring mass absorption spectrum of black carbons (MAC_{BC}) and their enhancement factors (E_{MAC-BC})^{23,24}. These anthropogenic carbons absorb significant amount of energy/light which translates to increased parenchymal fluorescence noted during IMI(Figures 5 6). Our analysis indicated that lungs damaged by these light absorbing carbons not only emitted 800nm wavelength lights but showed emission of 700 nm NIR light as well (Figure 6). Even when the patients who do not undergo NIR tracer infusion, the anthracotic areas secondary to light absorbing carbons causes fluorescence (Figure 5) indicating paramount importance light absorbing properties of these compounds. Understanding the intrinsic characteristics of the anthracotic lungs is of paramount importance for the development of new tracers.

Furthermore, soot has been shown to induce a cycle of perpetual inflammation of the lung by causing apoptosis of antigen-presenting cells via double stranded DNA breaks leading

to activation of the adaptive immune system⁹. These inflammatory foci in turn attract immune cells (tumor associated macrophages) which express folate receptor (folate receptor beta)²⁵ and lead highly permeable tumor microenvironment vasculature leading to false accumulation of NIR tracers. (Figure 7).

Lung cancers are a heterogenous group of malignancies and are not necessarily always linked to tobacco exposure²⁶. Multiple literature reports have found association of increased lung cancer risk with chronic lung disease such as COPD, asthma, and interstitial lung disease^{27,28}. Recognizing smoking as a major confounder, our analysis investigated the fluorescence parameters in patients who had a known diagnosis of chronic lung disease and no reported smoking history. As expected, given the low direct anthropogenic exposure, these patients had visibly low anthracosis. While not reaching statistical significance, there was a trend towards higher parenchymal fluorescence with duration of patient disease ($p=0.18$). These patients had higher normal parenchymal autofluorescence leading to higher MFI (287 vs 154, $p<0.01$) and decreased TBR measurements compared to those without chronic lung disease (2.11 vs 4.32, $p<0.05$). Interestingly, the lesion fluorescence was not different between the groups indicating that targeted NIR tracer localized to the tumors.

Anthracosis, lung inflammation, and lung disease have been found at a higher rate in those with who have increased levels of pollutant exposure²⁹⁻³¹. Naturally, this would be the case in urban dwellers compared to those who live in rural areas. We explored the AQI, particularly the PM_{2.5} levels corresponding to the zipcodes of the cohort. PM_{2.5} refers to fine inhalable particles, with diameters that are generally 2.5 micrometers and smaller. These particles come in many sizes and shapes and can be made up of hundreds of different chemicals. Some are emitted directly from a source, such as construction sites, unpaved roads, fields, smokestacks or fires. Most particles form in the atmosphere as a result of complex reactions of chemicals such as sulfur dioxide and nitrogen oxides, which are pollutants emitted from power plants, industries, and automobiles³²⁻³⁴. Previous epidemiological studies have indicated that ambient PM_{2.5} is carcinogenic and may increase the morbidity and mortality rates associated with lung cancer and PM_{2.5} has been suggested to decrease the survival time of patients with lung cancer^{33,35}.

Patients in the city of Philadelphia had the worst AQI and highest PM_{2.5} exposure compared to those living outside of the city (Supplemental Figure 1). However, PM_{2.5} exposure levels did not translate to statistically different levels of anthracosis and background lung MFI between urban, suburban, and rural areas of Philadelphia metropolitan area. There was higher lung background MFI and anthracosis difference between those living in the city and those living near the coast (Figure 4) (Table 2). This phenomenon is likely related to commuting patterns of patients in the rural and suburban communities to the city centers for work, which is thought to expose them to similar PM_{2.5} levels. The location does not appear to be a significant predictor of the degree of anthracosis, and IMI background fluorescence compared to smoking history and chronic lung disease.

There are several limitations that need to be acknowledged in this study. This is a retrospective analysis of a heterogenous group of patients coming from diverse backgrounds and environmental exposures. Biases from various confounders such as degree of smoking

history, commuter trends from rural and suburban areas into the city, occupational exposure, and duration of chronic lung disease should be accounted. Despite this, this study demonstrated that there are group of patients who appear to have significant anthracosis leading to decreased efficacy of IMI guided resections. These patients should be further studied in a randomized controlled fashion as IMI is likely to become a significant tool in the armamentarium of the thoracic surgeon. Understanding the effects of social determinants of health on potential efficacy of the technology can allow for more transparent informed consent and curb expectations in patients with high-risk features.

Conclusion:

Anthracosis of the lungs presents a unique challenge during IMI guided lung resections as it appears that these patients have decreased NIR lesion fluorescence and significantly elevated background parenchymal fluorescence leading to poor tumor to background differentiation. Current smokers with greater than 10 PPY and those with chronic lung disease appear to have decreased lesion to background discrimination, significant anthracosis, and IMI efficacy. Current smokers with cumulative >10 PPY and those with >10 PPY history who quit less than 10 years ago should be appropriately counselled regarding the expectations with IMI guided resections. These patients given the inability to clearly localize lesions can be subject to large segment resections and/or conversion to open thoracotomies for better tactile feedback which should be thoroughly discussed in the pre-operative informed consent process.

Supplementary Material

Refer to Web version on PubMed Central for supplementary material.

Acknowledgements:

Drs Azari, Kennedy, Singhal, contributed to the design and implementation of the research, to the analysis of the results and to the writing of the manuscript. Mr. Zhang, Ms Bernstein, Ms Chang, Mr. Nadeem, and Ms. Segil contributed to data collection and analysis of results. Drs Delikatny, Desphande, and Kucharczuk contributed to writing and reviewing of the manuscript.

Funding:

Dr. Azari was supported by the training grant in Surgical Oncology (T32) and the Society of Thoracic Surgeons. Dr. Kennedy was supported by the American Philosophical Society and the National Institutes of Health (grant F32 CA254210-01). Dr. Singhal was supported by the National Institutes of Health (NIH R01 CA193556) and the State of Pennsylvania Health Research Formula Fund.

References:

1. Lackey A & Donington JS Surgical Management of Lung Cancer. *Semin Intervent Radiol* 30, 133–140 (2013). [PubMed: 24436529]
2. Safdie FM, Sanchez MV & Sarkaria IS Prevention and management of intraoperative crisis in VATS and open chest surgery: how to avoid emergency conversion. *J Vis Surg* 3, 87 (2017). [PubMed: 29078649]
3. Azari F, Kennedy G & Singhal S Intraoperative Detection and Assessment of Lung Nodules. *Surgical Oncology Clinics* 29, 525–541 (2020). [PubMed: 32883456]

4. Predina JD et al. A Phase I Clinical Trial of Targeted Intraoperative Molecular Imaging for Pulmonary Adenocarcinomas. *Ann. Thorac. Surg* 105, 901–908 (2018). [PubMed: 29397932]
5. Newton AD, Predina JD, Nie S, Low PS & Singhal S Intraoperative fluorescence imaging in thoracic surgery. *J Surg Oncol* 118, 344–355 (2018). [PubMed: 30098293]
6. Azari F et al. Intraoperative molecular imaging clinical trials: a review of 2020 conference proceedings. *JBO* 26, 050901 (2021). [PubMed: 34002555]
7. Gutowski M et al. SGM-101: An innovative near-infrared dye-antibody conjugate that targets CEA for fluorescence-guided surgery. *Surgical Oncology* 26, 153–162 (2017). [PubMed: 28577721]
8. Predina JD et al. A Clinical Trial of TumorGlow to Identify Residual Disease During Pleurectomy and Decortication. *Ann Thorac Surg* 107, 224–232 (2019). [PubMed: 30028985]
9. Russell DW & Blalock JE The soot of all evil. *Elife* 4, e11709 (2015). [PubMed: 26488542]
10. Jamaati H et al. Multi-Gene Expression in Anthracosis of the Lungs as One of the Risk Factors for Non-Small Cell Lung Cancer. *Asian Pac J Cancer Prev* 18, 3129–3133 (2017). [PubMed: 29172290]
11. Nakamura S, Goto M & Chen-Yoshikawa TF Fluorescence-guided thoracic surgery. *Journal of Visualized Surgery* 7, (2021).
12. Hatier J-HB, Clearwater MJ & Gould KS The Functional Significance of Black-Pigmented Leaves: Photosynthesis, Photoprotection and Productivity in *Ophiopogon planiscapus* 'Nigrescens'. *PLOS ONE* 8, e67850 (2013). [PubMed: 23826347]
13. O'Shannessy DJ et al. Folate receptor alpha expression in lung cancer: diagnostic and prognostic significance. *Oncotarget* 3, 414–425 (2012). [PubMed: 22547449]
14. DSouza AV, Lin H, Henderson ER, Samkoe KS & Pogue BW Review of fluorescence guided surgery systems: identification of key performance capabilities beyond indocyanine green imaging. *J Biomed Opt* 21, 080901 (2016). [PubMed: 27533438]
15. Lee JY-K et al. Intraoperative Near-Infrared Optical Imaging Can Localize Gadolinium-Enhancing Gliomas During Surgery. *Neurosurgery* 79, 856–871 (2016). [PubMed: 27741220]
16. [AirNow.gov. https://www.airnow.gov/.](https://www.airnow.gov/)
17. Ferrari-Light D, Geraci TC, Sasankan P & Cerfolio RJ The Utility of Near-Infrared Fluorescence and Indocyanine Green During Robotic Pulmonary Resection. *Front Surg* 6, (2019). [PubMed: 30949483]
18. Nagaya T, Nakamura YA, Choyke PL & Kobayashi H Fluorescence-Guided Surgery. *Front Oncol* 7, (2017). [PubMed: 28168165]
19. Bach PB et al. Variations in Lung Cancer Risk Among Smokers. *JNCI: Journal of the National Cancer Institute* 95, 470–478 (2003). [PubMed: 12644540]
20. Mirsadraee M Anthracosis of the Lungs: Etiology, Clinical Manifestations and Diagnosis: A Review. *Tanaffos* 13, 1–13 (2014). [PubMed: 25852756]
21. Mirsadraee M & Saeedi P Anthracosis of Lung: Evaluation of Potential Underlying Causes. *Journal of Bronchology & Interventional Pulmonology* 12, 84–87 (2005).
22. Devarajan SR, Zarrin-Khameh N & Alapat P Black lungs and big nodes: A case of airway anthracosis with bronchial anthracofibrosis. *Respiratory Medicine Case Reports* 25, 9–11 (2018). [PubMed: 29892540]
23. Bond TC & Bergstrom RW Light Absorption by Carbonaceous Particles: An Investigative Review. *Aerosol Science and Technology* 40, 27–67 (2006).
24. Chakrabarty RK & Heinson WR Scaling Laws for Light Absorption Enhancement Due to Nonrefractory Coating of Atmospheric Black Carbon Aerosol. *Phys. Rev. Lett* 121, 218701 (2018). [PubMed: 30517814]
25. Tie Y et al. Targeting folate receptor β positive tumor-associated macrophages in lung cancer with a folate-modified liposomal complex. *Signal Transduction and Targeted Therapy* 5, 1–15 (2020). [PubMed: 32296011]
26. Smolle E & Pichler M Non-Smoking-Associated Lung Cancer: A Distinct Entity in Terms of Tumor Biology, Patient Characteristics and Impact of Hereditary Cancer Predisposition. *Cancers (Basel)* 11, 204 (2019). [PubMed: 30744199]

27. Choi W-I, Park SH, Park BJ & Lee CW Interstitial Lung Disease and Lung Cancer Development: A 5-Year Nationwide Population-Based Study. *Cancer Res Treat* 50, 374–381 (2018). [PubMed: 28494537]
28. Durham AL & Adcock IM The relationship between COPD and lung cancer. *Lung Cancer* 90, 121–127 (2015). [PubMed: 26363803]
29. Gao N et al. Lung function and systemic inflammation associated with short-term air pollution exposure in chronic obstructive pulmonary disease patients in Beijing, China. *Environmental Health* 19, 12 (2020). [PubMed: 32000783]
30. Jiang X-Q, Mei X-D & Feng D Air pollution and chronic airway diseases: what should people know and do? *J Thorac Dis* 8, E31–E40 (2016). [PubMed: 26904251]
31. Kurt OK, Zhang J & Pinkerton KE Pulmonary Health Effects of Air Pollution. *Curr Opin Pulm Med* 22, 138–143 (2016). [PubMed: 26761628]
32. Franklin M, Koutrakis P & Schwartz J The Role of Particle Composition on the Association Between PM_{2.5} and Mortality. *Epidemiology* 19, 680–689 (2008). [PubMed: 18714438]
33. Xing Y-F, Xu Y-H, Shi M-H & Lian Y-X The impact of PM_{2.5} on the human respiratory system. *J Thorac Dis* 8, E69–E74 (2016). [PubMed: 26904255]
34. US EPA, O. Particulate Matter (PM) Basics. <https://www.epa.gov/pm-pollution/particulate-matter-pm-basics> (2016).
35. Li R, Zhou R & Zhang J Function of PM_{2.5} in the pathogenesis of lung cancer and chronic airway inflammatory diseases. *Oncol Lett* 15, 7506–7514 (2018). [PubMed: 29725457]

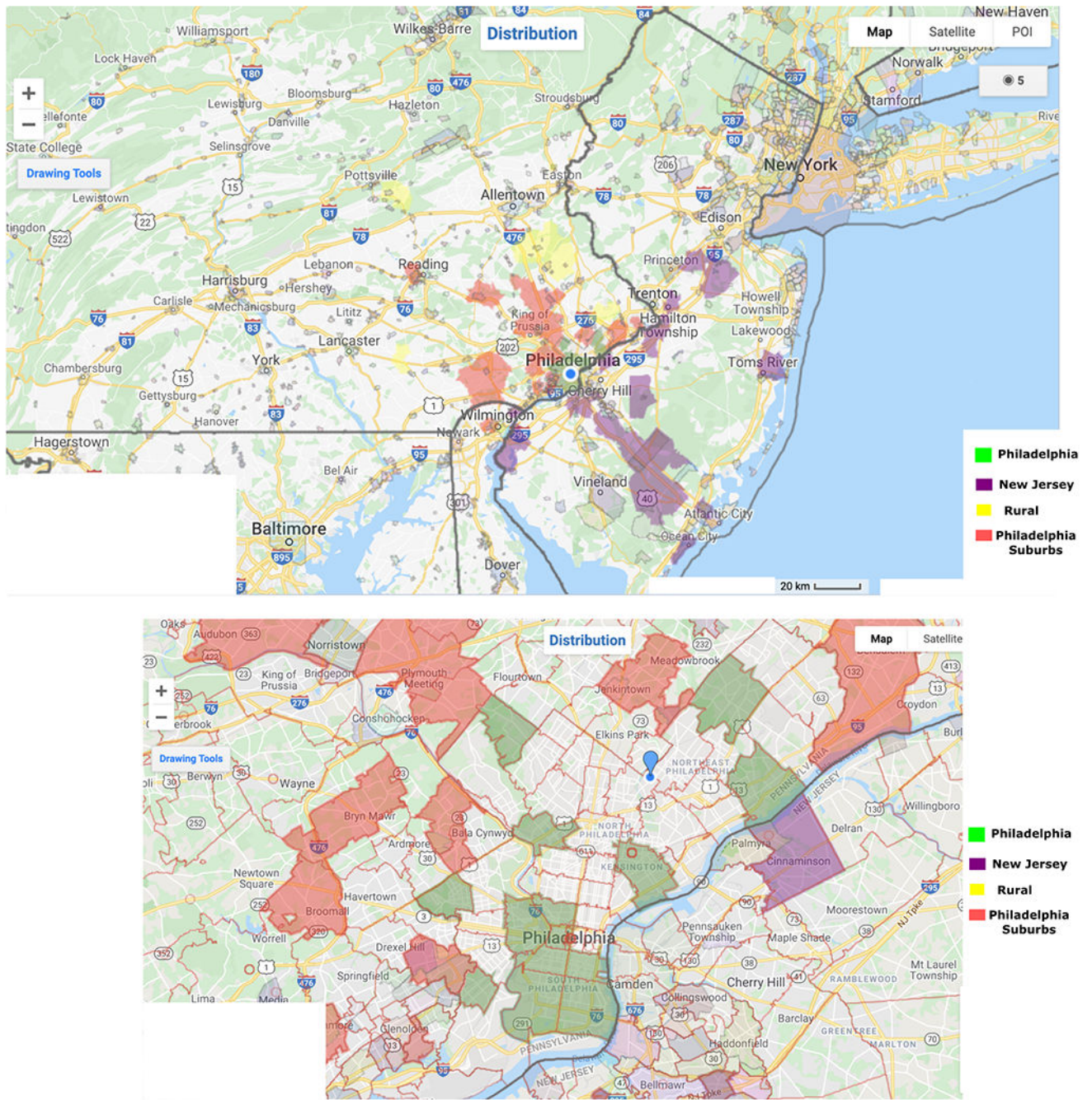


Figure 1:
Geographical distribution of the patient population in the study cohort.

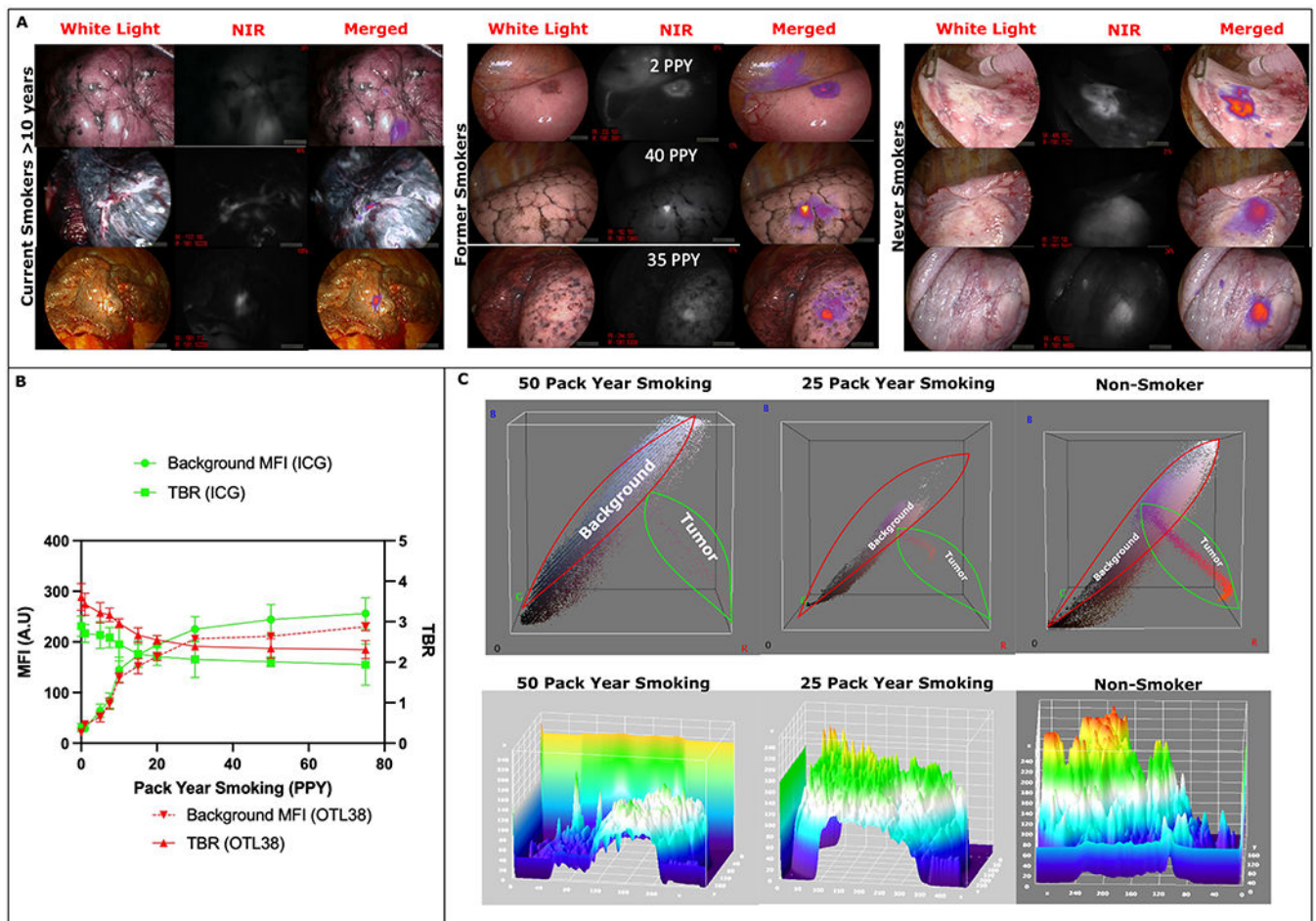


Figure 2:

(A): Left- Representative white light, NIR, and merged images from patients who were current smokers with >10 PPY at the time of surgery. As seen background lung parenchyma is significantly darker from smoke related inflammation leading to decreased contrast between tumor and background. Middle: representative images from past smokers showing background parenchymal inflammation are correlated with PPY. Right Representative images from never smokers showing minimal normal parenchyma inflammation and excellent contrast between normal lung and the tumor.

(B): Trend of background parenchymal intensity in relation to patient pack year smoking showing increased NIR fluorescence leading to lower TBR measurements in patients with higher smoking exposure.

(C): Top Row: 3D RGB analysis shows increased background color uptake than tumor fluorescence in patients with smoking history. Fused NIR images of tumors have increased Red color emission which is minimal in the 50 PPY group whereas Red color emission is significantly elevated in the non-smoker group highlighting increased tumor fluorescence and lower background detection.

Bottom Row: 3D Topographical heat map showing decreased tumor intensity compared to background lung parenchymal fluorescence (i.e increased background fluorescence

dampening tumor fluorescence intensity as detected by the device) in the smokers compared to non-smokers.

Author Manuscript

Author Manuscript

Author Manuscript

Author Manuscript

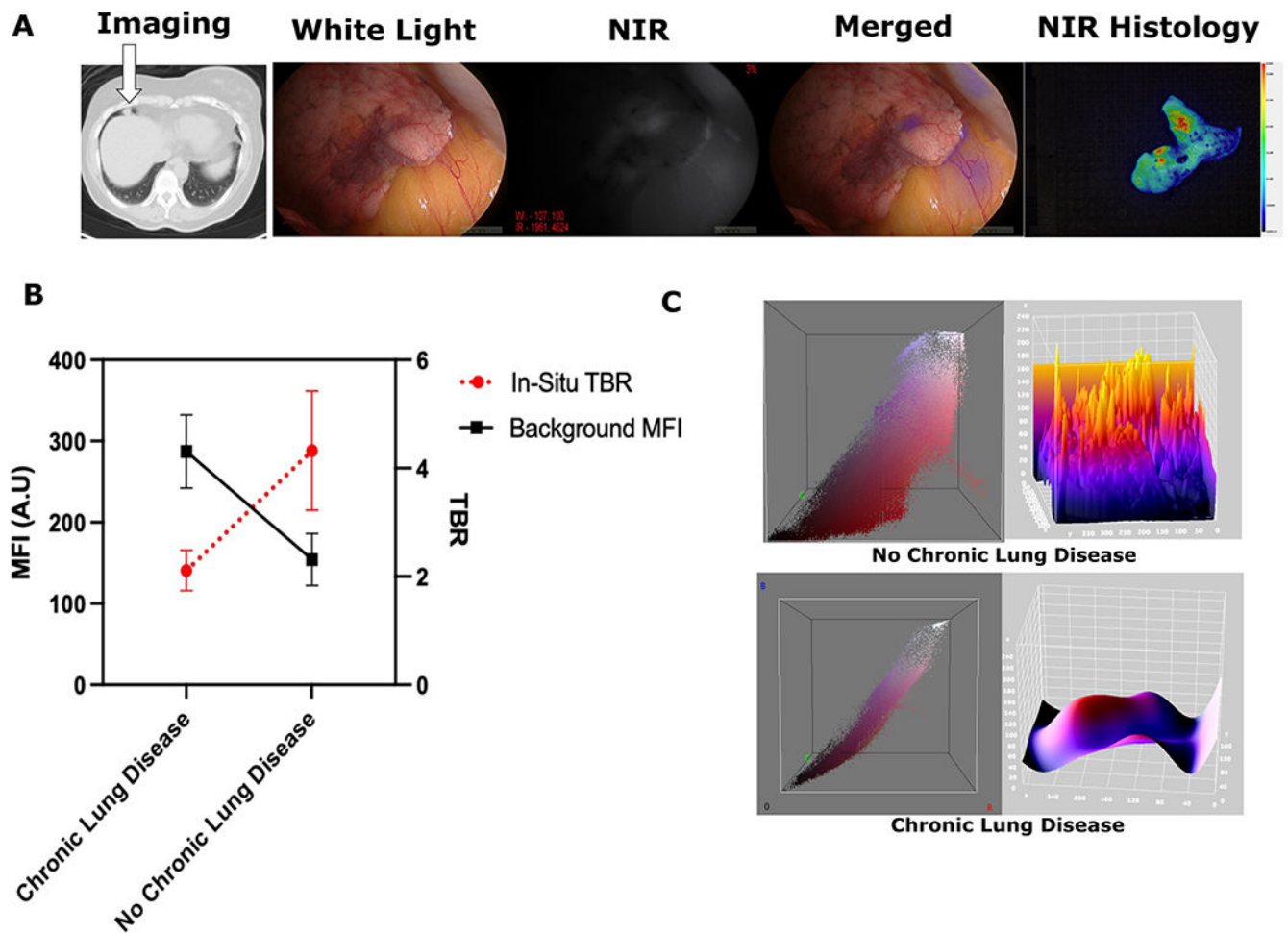


Figure 3:

(A): Sample images from IMI guided resection of lung lesion from a patient with 20 year history of chronic bronchitis. The lesion was hard to localize intra-operatively due to poor delineation from surrounding tissues, but IMI histology shows NIR tracer localization in the nodule. (B): Comparison of the background MFIs for Chronic Lung Disease patients vs those No Chronic Lung Disease shows increased background signal in those with chronic lung conditions ($p < 0.05$). Similar statistically significant observation was also noted for TBR measurements between the groups ($p < 0.05$) (C): Representative 3D analysis of an IMI guided resection showing increased fluorescence intensity in lung parenchyma in RGB and 3-D topographic analysis for chronic lung disease patients vs non chronic lung disease.

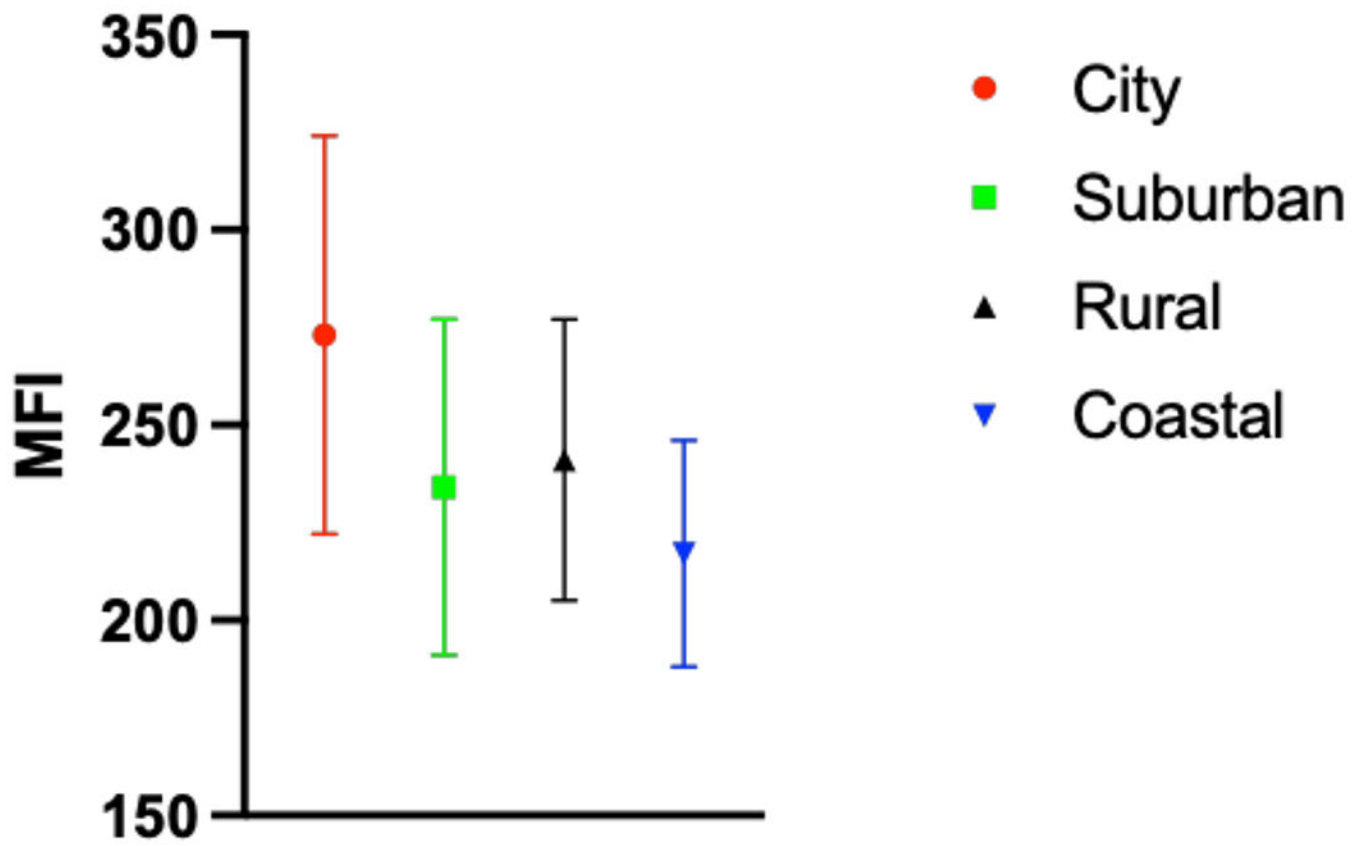


Figure 4:
Distribution of background parenchymal MFI based on patient domicile.

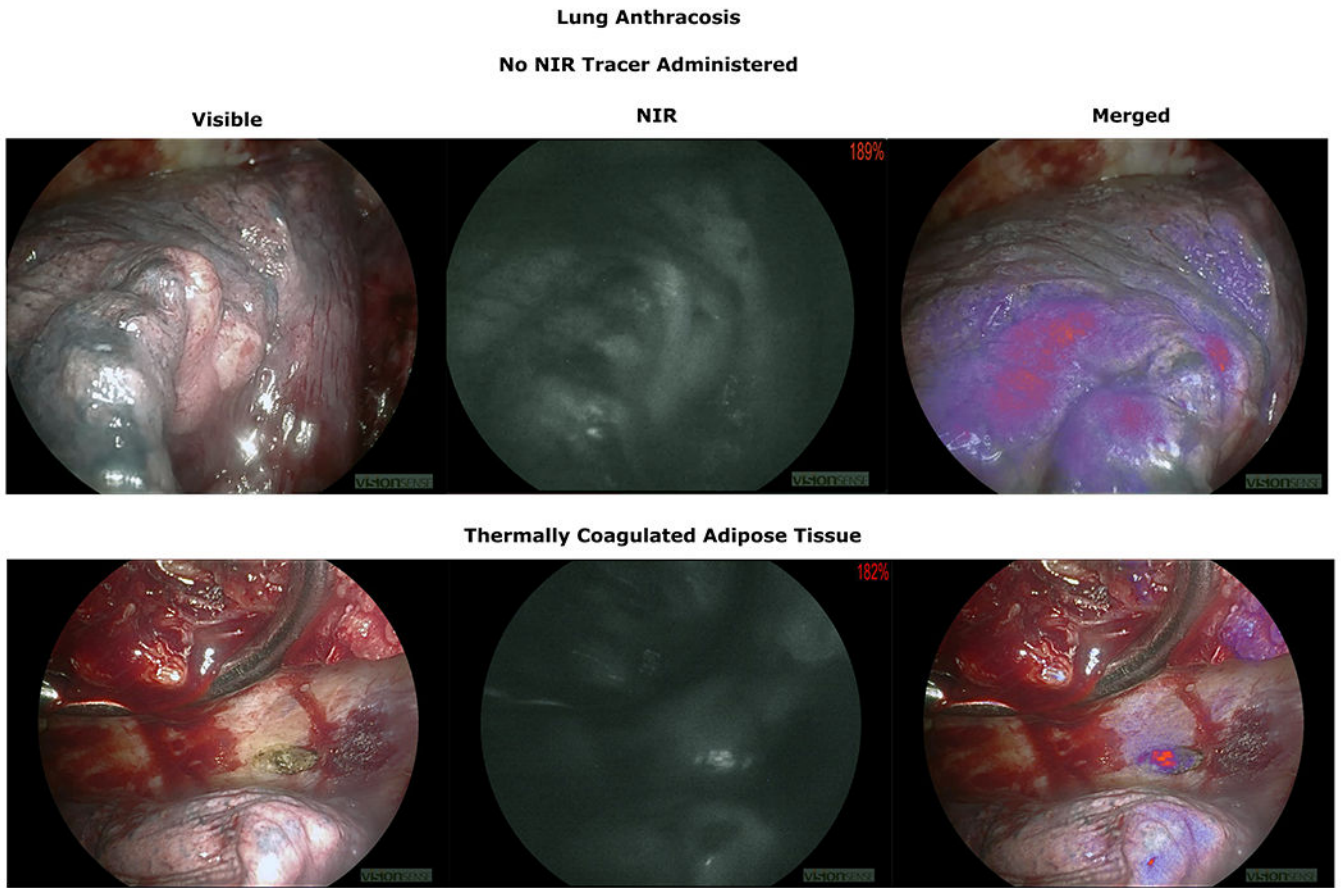


Figure 5:

Top Row: Demonstration of anthracotic lung parenchymal fluorescence in patients who did not receive any NIR infusion.

Bottom Row: Adipose tissue coagulated for hemostasis. Charred anthracotic area now shows NIR fluorescence.

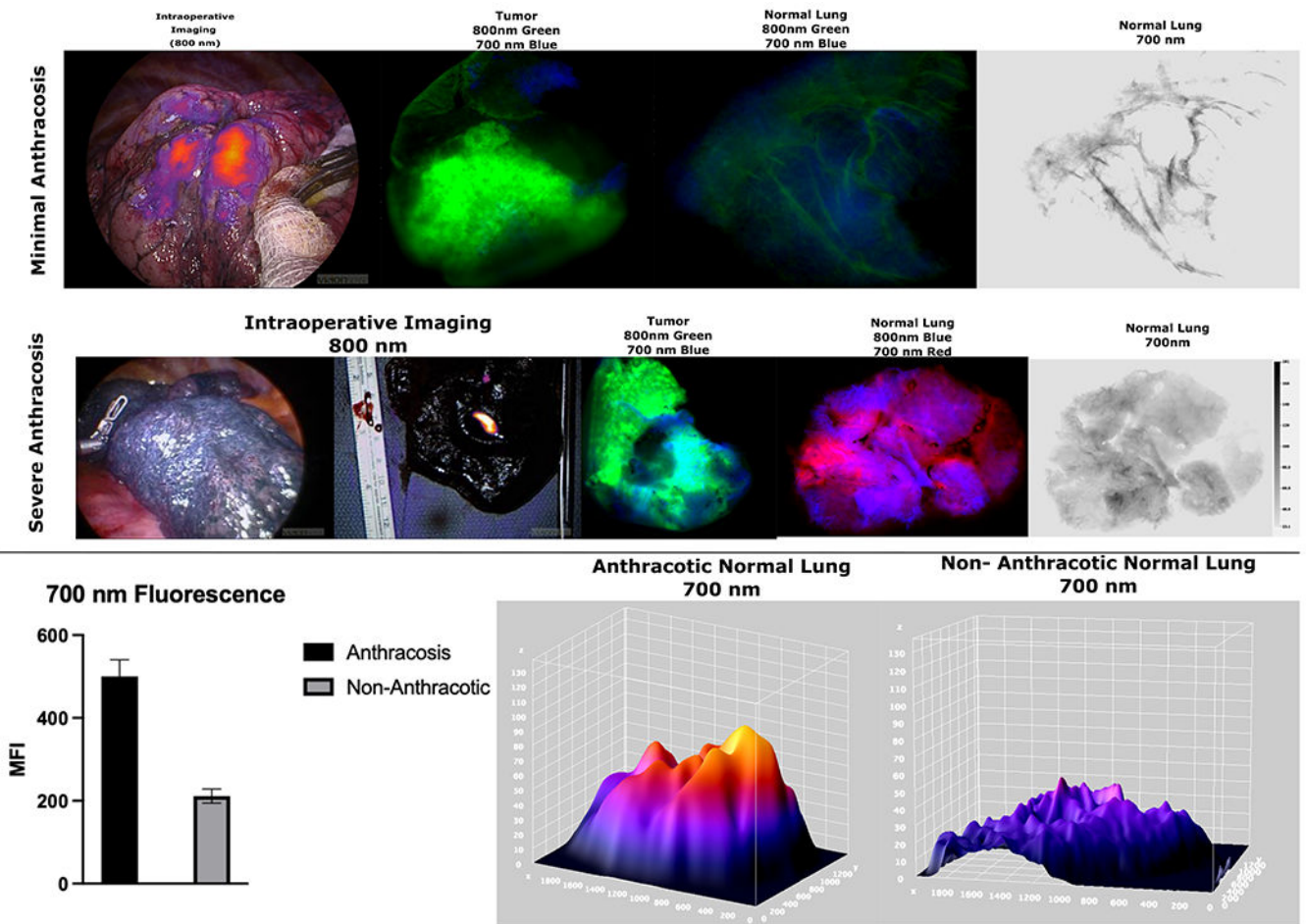


Figure 6:

Top Row: Specimen analysis of a minimally anthracotic lung during IMI guided cancer resection shows excellent tumor localization with ICG. Specimen analysis shows high tumor fluorescence in 800 nm wavelength with minimal background fluorescence and minimal fluorescence when analyzing the 700 nm wavelength emission.

Middle Row: Patient with severe anthracosis who underwent OTL38 guided lung cancer resection with specimen analysis showing very elevated fluorescence of normal tissue at 700 nm range. It should be noted that during in-vivo imaging during IMI, there was no fluorescence observed (left image) and lesion only fluoresced after the nodule was bisected demonstrating the limitations on tumor nodule fluorescence emission the anthracotic parenchyma presents

Bottom Row: Lungs with severe anthracosis due to light absorbing carbons showed statistically elevated emission at 700 nm ($p < 0.05$) with 3-D analysis showing elevated background MFI at those wavelengths as well.

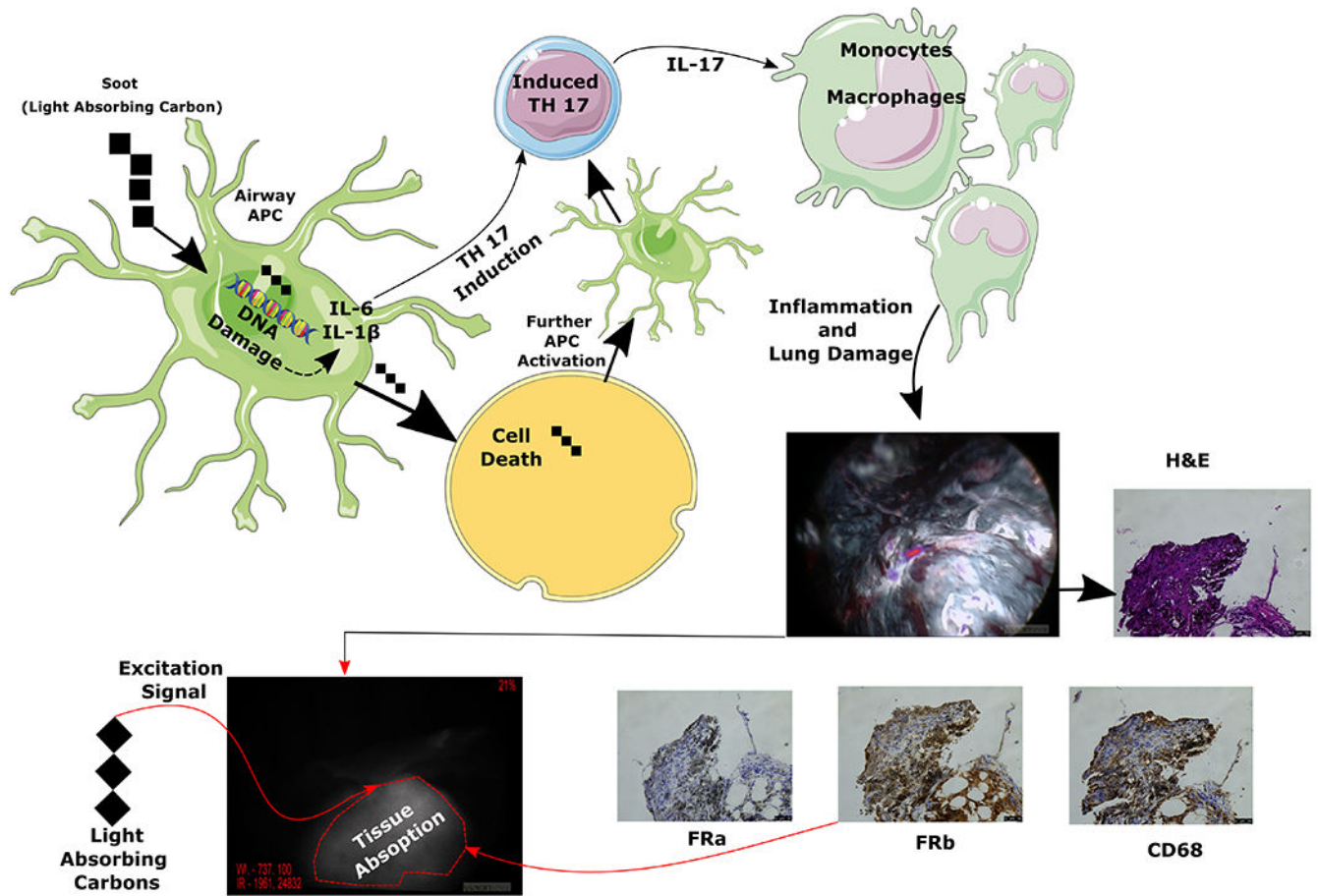


Figure 7: Pictorial representation of two mechanisms involved in anthracosis related background lung fluorescence. It is thought that soot (light absorbing carbons) gets taken up by antigen presenting cells (APC) which causes DNA breaks leading to cell death and induction of inflammatory cytokines which activated the adaptive immune system leading to inflammatory cascade. One of the cells that is recruited during this inflammatory response are the monocytes which become macrophages (see CD68 stain) and stain for folate receptor beta which is thought to bind folate targeted NIR tracers albeit at a lower degree. Additionally, soot because of its innate properties leads to black pigmentation and absorbs light/energy at a higher rate. Combination of these factors is thought to contribute to increased fluorescence of anthroctic lung tissue during IMI.

Table 1:

Demographic distribution of lung cancer cohort included in the study.

		Standard Deviation
Female n (%)	175 (62.5%)	
Male n (%)	104 (37.5%)	
ICG Guided Resections n (%)	74 (~26%)	
OTL38 Guided Resections n (%)	205 (~74%)	
Mean Age (Years)	64.1	12.8
Pack Year Smoking	30.5	35.1
Lesion Distance from Pleural Surface (cm)	0.61	0.11
Mean PET SUVmax	5.1	2.2
Median ASA	3	
Total Hospital Stay (days)	2.7	1.1
Any Smoking History (n)	147	
Never Smokers (n)	111	
History of Chronic Lung Disease Who Never Smoked (n)	46	
History of Any Chronic Lung Disease (Cohort) (n)	135	

Author Manuscript

Author Manuscript

Author Manuscript

Author Manuscript

Table 2:

Subset analysis of fluorescence parameters for patients who were diagnosed with adenocarcinoma of the lung.

	Overall Lung Adenocarcinoma Cohort Mean (STD)	Non-Anthroctic Lung Adenocarcinomas Mean (STD)	Anthracotic Lung Adenocarcinomas Mean (STD)
TBR (OTL38)	3.09 (0.55)	3.87 (0.91)	2.48 (0.43)
Background MFI (OTL38)	154 (27)	102 (17)	227 (36)
TBR (ICG)	2.44 (0.41)	2.67 (1.23)	2.11 (0.67)
Background MFI (ICG)	167 (34)	121 (21)	244 (39)

Author Manuscript

Author Manuscript

Author Manuscript

Author Manuscript

Table 3:

Fluorescence quantification based on patient location.

Location	Background MFI (SD)	Mean TBR (SD)
City	273 (51)	3.11 (0.71)
Suburban	234 (43)	3.32 (0.53)
Rural	241 (36)	3.44 (0.81)
Coastal	217 (29)	3.61 (0.61)

Author Manuscript

Author Manuscript

Author Manuscript

Author Manuscript